



Ultrafast ultrasound coupled with cervical magnetic stimulation for non-invasive and non-volitional assessment of diaphragm contractility

Thomas Poulard, Martin Dres, Marie-Cécile Nierat, Isabelle Rivals, Jean-Yves Hogrel, Thomas Similowski, Jean-Luc Gennisson, Damien Bachasson

► To cite this version:

Thomas Poulard, Martin Dres, Marie-Cécile Nierat, Isabelle Rivals, Jean-Yves Hogrel, et al.. Ultrafast ultrasound coupled with cervical magnetic stimulation for non-invasive and non-volitional assessment of diaphragm contractility. *The Journal of Physiology*, 2020, 598 (24), pp.5627-5638. 10.1113/JP280457 . hal-03266752

HAL Id: hal-03266752

<https://hal.sorbonne-universite.fr/hal-03266752>

Submitted on 22 Jun 2021

HAL is a multi-disciplinary open access archive for the deposit and dissemination of scientific research documents, whether they are published or not. The documents may come from teaching and research institutions in France or abroad, or from public or private research centers.

L'archive ouverte pluridisciplinaire **HAL**, est destinée au dépôt et à la diffusion de documents scientifiques de niveau recherche, publiés ou non, émanant des établissements d'enseignement et de recherche français ou étrangers, des laboratoires publics ou privés.

The Journal of Physiology

<https://jp.msubmit.net>

JP-TFP-2020-280457R2

Title: Ultrafast ultrasound coupled with cervical magnetic stimulation for non-invasive and non-volitional assessment of diaphragm contractility

Authors: Thomas Poulard
Martin Dres
Marie-Cécile Nierat
Isabelle Rivals
Jean-Yves Hogrel
Thomas Similowski
Jean-Luc Gennisson
Damien Bachasson

Author Conflict: Martin Dres: MD received personal fees from Lungpacer. Jean-Luc Gennisson: JLG is a scientific consultant for Supersonic Imagine, Aix-en-Provence, France.

Author Contribution: Thomas Poulard: Conception or design of the work; Acquisition or analysis or interpretation of data for the work; Drafting the work or revising it critically for important intellectual content; Final approval of the version to be published; Agreement to be accountable for all aspects of the work Martin Dres: Conception or design of the work; Drafting the work or revising it critically for important intellectual content; Final approval of the version to be published; Agreement to be accountable for all aspects of the work Marie-Cécile Nierat: Conception or design of the work; Drafting the work or revising it critically for important intellectual content; Final approval of the version to be published; Agreement to be accountable for all aspects of the work

Disclaimer: This is a confidential document.

Isabelle Rivals: Acquisition or analysis or interpretation of data for the work; Drafting the work or revising it critically for important intellectual content; Final approval of the version to be published; Agreement to be accountable for all aspects of the work Jean-Yves Hogrel: Conception or design of the work; Drafting the work or revising it critically for important intellectual content; Final approval of the version to be published; Agreement to be accountable for all aspects of the work Thomas Similowski: Conception or design of the work; Drafting the work or revising it critically for important intellectual content; Final approval of the version to be published; Agreement to be accountable for all aspects of the work Jean-Luc Gennisson: Conception or design of the work; Acquisition or analysis or interpretation of data for the work; Drafting the work or revising it critically for important intellectual content; Final approval of the version to be published; Agreement to be accountable for all aspects of the work Damien Bachasson: Conception or design of the work; Acquisition or analysis or interpretation of data for the work; Drafting the work or revising it critically for important intellectual content; Final approval of the version to be published; Agreement to be accountable for all aspects of the work

Running Title: Ultrafast ultrasound imaging of the diaphragm

Dual Publication: No

Funding: Fondation EDF: Thomas Poulard, Jean-Yves Hogrel, Damien Bachasson, N/A; Association Francaise contre les Myopathies (Association Française contre les Myopathies): Thomas Poulard, Jean-Yves Hogrel, Damien Bachasson, N/A The PhD fellowship of TP is funded by the Fondation EDF that is supporting the RespiMyo project, which includes the current study. This study was also supported by the Association Française Contre Les Myopathies (AFM).

Ultrafast ultrasound coupled with cervical magnetic stimulation for non-invasive and non-volitional assessment of diaphragm contractility

Thomas Poulard^{1,2}, Martin Dres^{3,4}, Marie-Cécile Niérat³, Isabelle Rivals⁵, Jean-Yves Hogrel², Thomas Similowski^{3,4}, Jean-Luc Gennisson^{1#}, Damien Bachasson^{2#*}

equally contributing authors

¹ Laboratoire d'Imagerie Biomédicale Multimodale, BioMaps, Université Paris-Saclay, CEA, CNRS UMR 9011, Inserm UMR1281, SHFJ, 4 place du général Leclerc, 91401, Orsay, France

² Institute of Myology, Neuromuscular Investigation Center, Neuromuscular Physiology Laboratory, Paris, France

³ Sorbonne Université, INSERM, UMRS1158 Neurophysiologie respiratoire expérimentale et clinique, Paris, France

⁴ AP-HP. Sorbonne Université, Hôpital Pitié-Salpêtrière, Service de Pneumologie, Médecine intensive – Réanimation (Département "R3S"), F-75013, Paris, France

⁵ Equipe de Statistique Appliquée, ESPCI Paris, PSL Research University, UMRS 1158, 10 rue Vauquelin, 75005, Paris, France

*Corresponding author: Damien Bachasson, PhD. Institut de Myologie, Laboratoire de Physiologie et d'Evaluation Neuromusculaire, Hôpital Universitaire Pitié Salpêtrière, Paris 75651 Cedex 13, France. Tel: +33 1 42 16 66 41; fax: +33 1 42 16 58 81. E-mail: d.bachasson@institut-myologie.org

25 **Table of contents categories**

26 Respiratory

27

28 **Key points summary**

- 29 • Twitch transdiaphragmatic pressure elicited by cervical magnetic stimulation of the
30 phrenic nerves is a fully non-volitional method for assessing diaphragm contractility
31 in humans, yet it requires invasive procedures such as esophageal and gastric catheter-
32 balloons.
- 33 • Ultrafast ultrasound enables a very high frame rate allowing the capture of transient
34 events, such as muscle contraction elicited by nerve stimulation (twitch). Whether
35 indices derived from ultrafast ultrasound can be used as an alternative to the invasive
36 measurement of twitch transdiaphragmatic pressure is unknown.
- 37 • Our findings demonstrate that maximal diaphragm tissue velocity assessed using
38 ultrafast ultrasound following cervical magnetic stimulation is reliable, sensitive to
39 change in cervical magnetic stimulation intensity, and correlates to twitch
40 transdiaphragmatic pressure.
- 41 • This approach provides a novel fully non-invasive and non-volitional tool for the
42 assessment of diaphragm contractility in humans.

Abstract

Measuring twitch transdiaphragmatic pressure ($P_{di_{tw}}$) elicited by cervical magnetic stimulation (CMS) is considered as a reference method for the standardized evaluation of diaphragm function. Yet, the measurement of P_{di} requires invasive esophageal and gastric catheter-balloons. Ultrafast ultrasound is a non-invasive imaging technique enabling frame rates high enough to capture transient events such as evoked muscle contractions. This study investigated relationships between indices derived from ultrafast ultrasounds and $P_{di_{tw}}$, and how these indices may be used to estimate $P_{di_{tw}}$. CMS was performed in 13 healthy volunteers from 30 to 100 % of stimulator intensity in units of 10 % in a randomized order. $P_{di_{tw}}$ was measured and the right hemidiaphragm was imaged using a custom ultrafast ultrasound sequence with 1 kHz framerate. Maximal diaphragm axial velocity ($V_{di_{max}}$) and diaphragm thickening fraction ($TF_{di_{tw}}$) were computed. Intra-session reliability was assessed. Repeated-measures correlation (R) and Spearman correlation coefficients (ρ) were used to assess relationships between variables. Intra-session reliability was strong for $P_{di_{tw}}$ and $V_{di_{max}}$ and moderate for $TF_{di_{tw}}$. $V_{di_{max}}$ correlated with $P_{di_{tw}}$ in all subjects ($0.64 < \rho < 1.00$, $R = 0.75$; all $p < 0.05$). $TF_{di_{tw}}$ correlated with $P_{di_{tw}}$ in 8 subjects only ($0.85 < \rho < 0.93$, $R = 0.69$; all $p < 0.05$). Coupling ultrafast ultrasound and CMS show promise for the non-invasive and fully non-volitional assessment of diaphragm contractility. This approach opens up prospects for both diagnosis and follow-up of diaphragm contractility in clinical populations.

Key Words: Diaphragm, ultrafast ultrasound imaging, cervical magnetic stimulation, skeletal muscle, contractility, phrenic nerves

Introduction

Sixty years ago, [Agostoni & Rahn, \(1960\)](#) introduced a novel method to measure the specific contribution of the diaphragm to the intrathoracic pressure generated during inspiratory efforts, namely, transdiaphragmatic pressure (Pdi). Pdi is defined as the difference between gastric (Pga) and esophageal (Pes) pressures measured using gastric and esophageal probes. Twitch Pdi (Pdi_{tw}) elicited by cervical magnetic stimulation (CMS) was introduced 30 years ago and is considered as a reference method for the non-volitional assessment of diaphragm contractility ([Similowski et al., 1989](#)). Yet, measuring Pdi_{tw} is considered invasive and requires a high level of expertise ([Laveneziana et al., 2019](#)). Twitch mouth pressure (Pmo_{tw}) or nasal mask twitch pressure have been developed as an alternative to Pdi_{tw} ([Yan et al., 1992](#); [Teixeira et al., 2007](#)). However, this approach requires some degree of cooperation from the subjects because small inspiratory/expiratory efforts ([Similowski et al., 1993](#); [Hamnegard et al., 1995](#); [Windisch et al., 2005](#); [Kabitz et al., 2007](#)) are required prior the stimulation to prevent upper airway collapse and/or glottis closure and ensure adequate transmission. Moreover, these procedures required proper mouth occlusion, which cannot be performed in many patients such as patients with neuromuscular disorders.

Ultrasound (US) imaging has emerged as a tool for assessing the diaphragm ([Ueki et al., 1995](#)) and is increasingly used in clinical settings such as the intensive care unit ([Dres & Demoule, 2020](#)). Imaging of the zone of apposition of the right-hemidiaphragm is classically performed to investigate diaphragm behavior. Various indices can be derived from diaphragm US such as diaphragm excursion or thickening fraction ([Goligher et al., 2015](#); [Tuinman et al., 2020](#)), diaphragm strain ([Oppersma et al., 2017](#)), or more recently changes in diaphragm stiffness assessed with US shear wave elastography ([Bachasson et al., 2019](#)). However, these methods offer limited frame rate (i.e. a few tens of frames per second for standard US and a few frames per second for US shear wave elastography). Therefore, these methods cannot be used for capturing fast transient phenomena, such as diaphragm response elicited by CMS (~300 ms).

Ultrafast US is a fairly recent imaging technique enabling very high frame rates (up to 20 kHz, ([Sandrin et al., 1999](#))). This technique has previously been used in the biceps

brachii to visualize muscle behavior during short-lasting contractions ([Deffieux et al., 2008](#); [Gronlund et al., 2013](#)). By performing a radio frequency-based speckle tracking, ultrafast US allows the quantification of transient velocities of mechanical waves induced by transcutaneous electrical stimulation ([Deffieux et al., 2008](#)). Maximal tissue velocity has been reported to increase linearly with stimulation intensity. However, the relationship between tissue velocity and the force generated by the muscle during stimulation is unknown. In a recent pilot work, we reported that diaphragm response elicited by CMS can be imaged using ultrafast US and that responses elicited at high and low stimulation intensity can be discriminated ([Bachasson et al., 2018](#)). However, the relationship between diaphragm pressure generation and indices derived from ultrafast US during CMS remains to be thoroughly investigated.

Therefore, this study aimed at imaging the diaphragm during CMS at different intensity levels using ultrafast US. By investigating the relationships between $P_{di\text{tw}}$ and indices derived from ultrafast US imaging (i.e. thickening fraction, maximal tissue velocity), we hypothesized that diaphragm thickening fraction and diaphragm tissue velocity following CMS were correlated to $P_{di\text{tw}}$, and that these indices may be used as a surrogate to $P_{di\text{tw}}$.

Methods

Ethical approval

This study conformed to the Declaration of Helsinki. It was approved by the local ethics committee (Comité de Protection des Personnes Île-de-France VI, France, February 22nd 2016, ID-RCB 2015-A00949-40) and was publicly registered before the first inclusion (ClinicalTrials.gov, NCT03313141). All participants gave written informed consent. Some of the data from this study have already been published elsewhere, regarding the use of diaphragm shear wave elastography in healthy subjects during ventilation ([Bachasson et al., 2019](#)).

Participants

Thirteen healthy participants (5 males and 8 females, median (Q1-Q3) – age = 24 (22-27) years, height = 171 (167-183) cm, BMI = 20.6 (19.7-22.6) kg.m⁻²) were studied. Participants had to be 18 and over with no history of respiratory or neuromuscular disorders, and no contraindication to CMS ([Rossi et al., 2011](#)).

Pressure measurements

Participants were studied in a semirecumbent position (~45 degrees) with uncast abdomen. Pes and Pga were measured using 8 cm balloon catheters (Marquat Genie Biomedical, Boissy-Saint-Léger Cedex, France). Balloons were introduced through the participant's nostril and both placed in the stomach so that a positive pressure deflection was monitored when gently pressing the participant's stomach. Subsequently, one balloon was slowly withdrawn toward the esophagus until the pressure deflection was no more monitored when pressing the participant's stomach, and was then withdrawn an additional 10 cm. Esophageal balloon position was adjusted using the Baydur maneuver ([Baydur et al., 1982](#)). Balloons were then connected to differential pressure transducers (MLT0380/D, ADInstruments, Bella Vista, Australia) and filled with 4 and 5.5 ml of air in the esophageal and gastric balloons, respectively ([Mojoli et al., 2015](#)). All signals were digitized at a 4 kHz frequency using a PowerLab system (16/35, ADInstruments, Bella Vista, Australia) and recorded on the LabChart software. Pdi was computed as the difference between Pga and Pes.

Cervical Magnetic Stimulation

CMS was performed using a Magstim 200 stimulator (Magstim, Whitland, Dyfed, UK) driving a 90-mm circular coil (1 Tesla maximum output) as previously described ([Similowski et al., 1989](#)). Briefly, participants were asked to bend their neck forward and the central hole of the coil was positioned on the spinous process of the seventh cervical vertebra. Optimal coil position was determined by performing a series of stimulation at 100 % of stimulator intensity. The spot where Pdi_{tw} was the highest was skin-marked and kept constant during the whole experiment.

Ultrafast ultrasound imaging

The zone of apposition of the right hemidiaphragm was imaged using a 6 MHz central frequency linear transducer (SL 10-2) driven by an ultrafast ultrasound device (Aixplorer V12, Supersonic Imagine, Aix-en-Provence, France). The probe was placed on the mid-axillary line, vertical to the chest wall, at the 8th-10th intercostal space. The site of the probe placement was skin-marked to ensure that the same region of interest was imaged during the whole protocol. The diaphragm was identified as a three-layers structure superficial to the liver, with two hyperechoic layers (*i.e.* the *pleura* and *peritoneum*) surrounding a hypoechoic muscular layer (Figure 1). As the duration of Pdi_{tw} is ~ 300 ms, a custom ultrafast US sequence was designed to track diaphragm movements during this time window. The sequence was composed of 9 plane-wave US with different angles (-7° to 7° with a 2° incremental steps) at 9 kHz frame rate, yielding a compounded frame rate of 1 kHz and a 500 ms ([Montaldo et al., 2009](#)). This sequence followed the Food and Drugs Administration guidelines for acoustics norms (Mechanical index = 0.5, Thermal index = 0.2). Because diaphragm depth rarely exceed 4 cm ([Shahgholi et al., 2014](#)), the US sequence was developed in order to maintain the same spatial and temporal resolution of to this depth of 4 cm. Such sequence allows the imaging of the diaphragm in overweight patients. Signals were synchronized using an output trigger sent from the ultrafast US device to the Powerlab system. A fixed delay of 100 ms was set between the onset of US recordings and CMS, after which the stimulator was triggered by the Powerlab for delivering the stimulation. Recording of pressure signals was started 1 s before the US trigger. The experimental setup and procedure for recording pressure and US frames is displayed in Figure 2. Of note, we investigated whether diaphragm excursion elicited by CMS may be imaged during subcostal scanning during pilot works. We measured very small excursion values that were highly variable between trials. This finding was expected as diaphragm response elicited by CMS is not associated with substantial change in pulmonary volume. This may be mainly explained by glottis closure. Consequently, the measurement of diaphragm excursion during CMS was not further explored.

Experimental protocol

Cervical magnetic stimulations. Participants were stimulated on the predefined optimal stimulation spot from 30 to 100 % of stimulator intensity in units of 10 %, in a randomized order. All stimulations were delivered at functional residual capacity (FRC). Lung volume prior stimulation, estimated through Pes, was checked to be consistent across all stimulations. A minimum of three stimulations, separated by at least one minute, were performed at each stimulation intensity. Two to three validated trials (i.e. as indicated by appropriate Pes before CMS) per intensity were considered for further analysis.

Maximal voluntary maneuvers. Participants were asked to perform maximal inspiratory effort at residual volume. Maximal Pdi ($P_{di_{max}}$) was measured using a unidirectional valve allowing expiration only. Participants were asked to empty their lungs before being strongly encouraged to generate maximal inspiratory effort. Visual feedback of Pdi was provided during the maneuver. Three to five trials were performed and maximal pressure measured over a 1 s period was recorded as $P_{di_{max}}$. Sniff nasal inspiratory pressure (SNIP) was determined as follows. Participants were asked to make a short and maximal sniff at FRC. As recommended ([American Thoracic Society/European Respiratory, 2002](#)), participants performed 8-10 attempts with a ~30-s rest in-between sniffs until a plateau of peak pressure values was reached.

Data analysis

All data were analyzed offline using standardized Matlab scripts (Mathworks, Natick, MA, USA). Pes, Pga, and Pdi signals were low-pass filtered (30 Hz) using a second-order Butterworth filter. Esophageal twitch pressure ($P_{es_{tw}}$), gastric twitch pressure ($P_{ga_{tw}}$), and $P_{di_{tw}}$ following stimulation were calculated as the difference between maximal (for Pdi and Pga) or minimal (for Pes) pressure and pressure at the onset of CMS.

Vertical speckle tracking was performed by computing the axial (i.e. perpendicular to the ultrasound probe) relative displacements within the diaphragm. This technique consists in comparing consecutive images using one-dimensional cross-correlations to measure the relative displacement of a pixel between two consecutive frames ([Loupas et al., 1995](#)). Diaphragm tissue velocity profile is then computed by dividing the measured displacement by the time difference between two frames (i.e. 1 ms). As an example, Figure 3 shows how

the velocity within the diaphragm evolves over time. Diaphragm velocity was computed over each column of pixels within the diaphragm. The central third of each image was then averaged to obtain a single value of diaphragm velocity over time. This value was assumed to be representative of the whole diaphragm. Maximal diaphragm velocity ($V_{di_{max}}$) was then determined as the maximal (i.e. positive) velocity within this signal.

For each trial, a time-motion image was generated using the central pixel line of each ultrasound image, referred to as M-Mode in the following. The position of the *pleura* and *peritoneum* layers was then drawn manually over the full length of the M-Mode image. By doing so, diaphragm thickness (i.e. the difference between the *peritoneum* and *pleura* positions) was computed at each time of the US acquisition. Maximal diaphragm thickening fraction ($TF_{di_{tw}}$) was computed using resting diaphragm thickness prior stimulation ($T_{di_{rest}}$) and maximal diaphragm thickness following stimulation ($T_{di_{max}}$) as follows:

$$TF_{di_{tw}} (\%) = \frac{T_{di_{max}} - T_{di_{rest}}}{T_{di_{rest}}} \times 100 \quad [1]$$

All $TF_{di_{tw}}$ measurements were performed by a single trained operator (TP), blinded to the stimulation intensity. A movie clip showing pressure signals, M-mode images, and indices derived from ultrafast US is available in supplementary materials S1.

Statistics

Results are presented as median (Q1-Q3) unless otherwise stated. Normality was assessed by visual inspection (*QQ plots* and density distributions) and by significance tests (*Shapiro-Wilk test*). Because all variables failed the normality test, Friedman repeated measures ANOVAs were used. ANOVAs were conducted to compare P_{es} prior to each stimulation at all stimulation intensities. Within-day reliability of $P_{di_{tw}}$, $V_{di_{max}}$, and $TF_{di_{tw}}$ was investigated. Standard errors of measurement (SEM) and intraclass correlation coefficients (ICC) were used to study absolute and relative reliability, respectively ([Hopkins, 2002](#)). The overall relationship between variables (R) was determined using repeated measure correlation ([Bakdash & Marusich, 2017](#)). This technique considers the independence of repeated measures between individuals, so that potential confounding factors, such as between-participant variability, do not interfere. Data are presented as R [95 % CI]. Spearman

correlation coefficients (ρ) were calculated to investigate within-individual relationships between variables. ANOVAs were used to assess the effect of stimulation intensity on Pdi_{tw} , Vdi_{max} , and $TFdi_{tw}$. Tukey's *post-hoc* tests were conducted if a significant main effect of intensity was found. Within individuals, Pdi_{tw} , Vdi_{max} , and $TFdi_{tw}$ were considered supramaximal if the average Pdi_{tw} , Vdi_{max} or $TFdi_{tw}$ at submaximal and maximal stimulation intensities was inferior or equal to the coefficient of variation of the variable at each stimulation intensities ([Welch et al., 2018](#); [Geary et al., 2019](#)). Supramaximality was reached if greater stimulation intensity did not result in further increase in Pdi_{tw} , Vdi_{max} or $TFdi_{tw}$. Analyses were performed in the computing environment R ([R Core Team, 2020](#)). Significance was set at $p < 0.05$ for all tests.

Results

All participants completed the protocol. Pdi_{max} was 113 (71-115) cmH₂O 90 (56-117) cmH₂O in men and women, respectively. Overall, Pdi_{max} was 108 (71-117) cmH₂O. SNIP was 116 (109-130) cmH₂O in men and 103 (90-118) cmH₂O in women. Overall, SNIP was 109 (96-123) cmH₂O. The one-way repeated measures ANOVA showed that Pes at the onset of CMS was similar across all stimulations at all intensities ($p = 0.2430$). Within-day SEM and ICC of Pdi_{tw} , Vdi_{max} , and $TFdi_{tw}$ are presented in Table 1. Typical B-Mode images over the course of the 500 ms US acquisition are presented in supplementary materials S2.

Effect of stimulation intensity on indices derived from ultrafast ultrasound

M-Mode images and temporal evolution of the displacements of the *pleura* and *peritoneum*, Vdi_{max} , and recorded pressures in one individual are displayed in Figure 4 (also see movie clip in Supporting Information S1). Pes_{tw} , Pga_{tw} , and Pdi_{tw} at all tested stimulation intensities are shown in Figure 5 and Figure 6A. Vdi_{max} and $TFdi_{tw}$ at all tested stimulation intensities are displayed in Figure 6B-C. Within individual relationships between stimulation intensity and Pdi_{tw} , Vdi_{max} , and $TFdi_{tw}$ are shown in Figure 6D-F.

Pdi_{tw} was significantly related to stimulation intensity in all subjects (ρ ranged from 0.83 to 1.00, all $p < 0.0100$; $R = 0.91$, 95 % CIs [0.86 0.94], $p < 0.0001$). At the group level, there was a significant main effect of stimulation intensity on Pdi_{tw} . *Post-hoc* tests indicated

that Pdi_{tw} significantly increased up to 100 % of stimulation intensity (all $p < 0.05$). Within individuals, Pdi_{tw} plateaued at 90 % of stimulation intensity in two participants. In other participants, Pdi_{tw} increased until 100 % of stimulation intensity.

Vdi_{max} correlated to stimulation intensity in all participants (ρ ranged from 0.79 to 1.00, all $p < 0.0500$; $R = 0.83$, 95 % CIs [0.75 0.89], $p < 0.0001$). At the group level, there was a significant main effect of stimulation intensity on Vdi_{max} . *Post-hoc* tests indicated that Vdi_{max} did not significantly differ between 90 and 100 % of stimulation intensity ($p = 0.9997$). No significant differences in Vdi_{max} was found between consecutive stimulation intensities, except between 80 and 90 % of stimulation intensity ($p = 0.0080$). Within individuals, Vdi_{max} plateaued at 90 % of stimulation intensity in 6 participants, at 80 % in one participant, and at 70 % in one participant.

$TFdi_{tw}$ correlated to stimulation intensity ($R = 0.72$, 95 % CIs [0.60 0.80], $p < 0.0001$). Individual correlations were significant in 10 out of 13 subjects (ρ ranged from 0.67 to 0.95, all $p < 0.05$; ρ ranged from 0.33 to 0.52 in the three remaining participants, all $p > 0.2200$). At the group level, there was a significant main effect of stimulation intensity on $TFdi_{tw}$. *Post-hoc* tests showed that $TFdi_{tw}$ did not significantly differ between 60 to 100% of stimulation intensity (all $p > 0.1155$). No significant differences in $TFdi_{tw}$ was found between consecutive stimulation intensities. Within individuals, $TFdi_{tw}$ plateaued at 90 % of stimulation intensity in 5 participants, at 80 % in two participants, at 70 % in two participants, at 50 % in one participant and at 30 % in one participant. $TFdi_{tw}$ and Vdi_{max} at all stimulation intensities are shown in Figure 6B and 6C, respectively.

Relationships between Pdi_{tw} and indices derived from ultrafast ultrasound

Within-individuals' relationships between Pdi_{tw} and Vdi_{max} , and between Pdi_{tw} and $TFdi_{tw}$ are presented in Figure 7. Vdi_{max} correlated to Pdi_{tw} in all participants (ρ ranged from 0.64 to 1.00, all $p < 0.05$; $R = 0.75$, 95 % CIs [0.65 0.83], $p < 0.0001$). $TFdi_{tw}$ positively correlated to Pdi_{tw} ($R = 0.69$, 95 % CIs [0.57 0.79], $p < 0.0001$) and individual correlation coefficients were significant in 8 out of 13 participants (ρ ranged from 0.85 to 0.93, all $p < 0.05$; ρ ranged from -0.27 to 0.70, in the five remaining participants, all $p > 0.06$).

Discussion

This study is the first to image the diaphragm contraction induced by CMS using ultrafast US. The main results are as follow: i) maximal tissue velocity within the diaphragm significantly increased with stimulation intensity while diaphragm thickening fraction plateaued at low stimulation intensity, ii) intra-session reliability of maximal tissue velocity within the diaphragm was high and intra-session reliability of diaphragm thickening fraction was poor iii) twitch transdiaphragmatic pressure strongly correlated with maximal tissue velocity within the diaphragm and moderately correlated with diaphragm thickening fraction.

Vdi_{max} is sensitive to changes in stimulation intensity and correlates to twitch transdiaphragmatic pressure

We found that Vdi_{max} increased with stimulation intensity in all participants. These results are in line with previous works that reported a gradual increase in tissue velocity with stimulation intensity during contractions elicited in the *biceps brachii* ([Deffieux et al., 2008](#); [Gronlund et al., 2013](#)). To the best of our knowledge, this study is the first to report the relationship between a muscle's tissue velocity and the force/pressure it produces. We found that Vdi_{max} correlated to Pdi_{tw} in all participants, supporting that the magnitude of Vdi_{max} is associated with the diaphragm contractility. Interestingly, Pdi_{tw} was supramaximal in two subjects only, whereas Vdi_{max} was supramaximal in 8 subjects. The inability to reach supramaximal Pdi_{tw} values in some subjects has been addressed before ([Man et al., 2004](#); [Spiesshoefer et al., 2019](#)). This may be partly explained by insufficient magnetic stimulation power to fully activate the phrenic nerves. It cannot be ruled out that supramaximality of Pdi_{tw} occurred between 90 and 100 % of stimulation intensity. Nonetheless, it is known that CMS at highest stimulation intensities stimulates neck muscles ([Attali et al., 1997](#)). Thus, Pdi_{tw} is likely to increase not because of a higher activation of the diaphragm, but because the recruitment of neck muscles increases the deflation of twitch Pes ([Wragg et al., 1994](#); [Laghi et al., 1996](#)). Regarding Vdi_{max}, supramaximality was reached in 8 out of 13 participants. The fact that Vdi_{max} plateaued while Pdi_{tw} continued to increase may be related to specificity of Vdi_{max} measurement, which directly probe the diaphragm. Therefore, Vdi_{max} may be considered as a specific index of diaphragm contractility following CMS, ruling out

the confounding effects related to the recruitment of extra diaphragmatic muscle. $V_{di_{max}}$ did not meet supramaximality criteria in 5 subjects. Interestingly, 4 out of these 5 subjects did not reach supramaximality for $P_{di_{tw}}$ either. It can thus be suggested that the absence of $V_{di_{max}}$ supramaximality is directly related to the absence of $P_{di_{tw}}$ supramaximality. Also, one may observe that V_{di} increases in the milliseconds following stimulation, while P_{di} peaks ~ 150 ms after stimulation (Figure 4). This supports that the rapid change in V_{di} correspond to diaphragm contraction and that this lag reflects the time needed for the diaphragm to transfer its force generation into an actual pressure generation. Importantly, $V_{di_{max}}$ was found to be strongly reproducible, as indicated by low SEM and high ICC that were comparable to those observed for $P_{di_{tw}}$ (Table 1). This high reliability build confidence regarding the potential of $V_{di_{max}}$ for non-volitional monitoring of diaphragm contractility over time. This study is also the first to report $TF_{di_{tw}}$ values during CMS. Repeated measure correlations showed a significant correlation between $TF_{di_{tw}}$ and stimulation intensity. Within individuals, 10 (77 %) participants presented with a significant relationship between $TF_{di_{tw}}$ and stimulation intensity. As compared to $V_{di_{max}}$, $TF_{di_{tw}}$ was shown to be less sensitive to changes in stimulation intensity. At the group level, $TF_{di_{tw}}$ was moderately correlated to $P_{di_{tw}}$. Our results are in line with previous studies that reported significant relationship between diaphragm thickening fraction and changes in P_{di} during spontaneous breathing, inspiratory efforts, or in mechanically ventilated patients ([Ueki et al., 1995](#); [Vivier et al., 2012](#); [Goligher et al., 2015](#); [Umbrello et al., 2015](#)). However, when looking at individual relationship, the correlation between $TF_{di_{tw}}$ and $P_{di_{tw}}$ reached significance in 8 subjects (62%) only. We also found that $TF_{di_{tw}}$ plateaued at low stimulation intensity (60%). Importantly, the intra-session reliability of $TF_{di_{tw}}$ was rather poor. There are several potential explanations for these findings. First, $TF_{di_{tw}}$ was computed manually by drawing the position of the *pleura* and *peritoneum*. Imprecisions during this manual step might also be amplified by the lower image quality found using ultrafast US as compared to that of conventional US imaging. More specifically, conventional US imaging uses focused pulses, allowing for high image quality but a relatively low sampling rate (a few tens per second). On the other hand, ultrafast US plane wave imaging allows very high sampling rate (here, 1 kHz) but image quality is lower ([Montaldo et al., 2009](#)). Indeed, ultrafast US prevents the focusing of US beams to a specific

tissue (i.e. in this case, the diaphragm) and negatively impacts the signal to noise ratio of the resulting image. As a result, the ultrafast US sequence developed for the current experiment does not allow strong contrast of anatomic structures in comparison to standard US imaging (Figure 1A). This may disrupt the measurement of $TFdi_{tw}$ (Figure 1B) and contribute to explain the low intra-session reliability of $TFdi_{tw}$ indicated by the substantial SEM (~10%) and moderate ICC (<0.6). Noteworthy, $TFdi$ during ventilation was previously shown to be moderately reliable using traditional ultrasound imaging ([Goligher et al., 2015](#)). This low reliability may explain, at least in part, the absence of increase in $TFdi_{tw}$ with increasing stimulation intensity and increasing Pdi_{tw} in some participants. Indeed, we found in some participants that $TFdi_{tw}$ plateaued at intensities as low as 40—60 %. Because of the large increase in Pdi_{tw} between 60 and 100 % of stimulation intensity, it is very unlikely that supramaximal $TFdi_{tw}$ values depicts full diaphragm recruitment. All together, these findings suggest that $TFdi_{tw}$ may be of limited help to assess diaphragm contractility in response to CMS.

Perspectives and limitations

We demonstrated that Vdi_{max} was strongly related to Pdi_{tw} in all subjects. This could have important implications for monitoring temporal changes in diaphragm contractility in patients presenting with diaphragm dysfunction. In other words, Vdi_{max} elicited by CMS could be monitored over time using ultrafast US, allowing iterative, specific, fully non-invasive and non-volitional assessment of diaphragm contractility. It is worth noting that between-subject variability was relatively important. In turn, one may question how Vdi_{max} may be used to identify diaphragm dysfunction. Further studies will focus on this specific point, with the perspective that Vdi_{max} may be one parameter, among others, guiding clinicians through the assessment of diaphragm contractility. Inter-operator and between day reliability of Vdi_{max} remains to be investigated. Assessing the delay between CMS and diaphragm response as assessed using Vdi_{max} may also be promising to investigate both phrenic conduction and electromechanical delay. Unfortunately, EMG was not available in the current study and this shall be investigated in future works. As mentioned above, we cannot ensure that supramaximality was achieved in all subjects. It is possible that

maximality occurred between 90 and 100 % of stimulation intensity in some subjects. This problem has been addressed before ([Man et al., 2004](#); [Spiesshoefer et al., 2019](#)), but can be considered negligible if a rigorous and standardized study-design is routinely used. Also, as the primary aim of this study was to detect changes in diaphragm contractility according to stimulation intensity and relationships between variables, supramaximality should not be considered as an important concern. We also emphasize that only the right hemidiaphragm was imaged in this study and that future works shall thoroughly investigate this approach in the left hemidiaphragm. Lastly, the ultrafast US sequence used in this study was custom-made so that the present approach cannot be readily generalized to clinical environments as it required a specific US scanner, US sequences that are not available commercially, specific training, and represent a non-negligible costs.

Conclusion

These study shows that ultrafast US may be used to image diaphragm behavior following CMS. Diaphragm tissue velocity is strongly correlated with twitch transdiaphragmatic pressure and appears to be highly specific to diaphragm contractility. Further research is warranted to investigate how ultrafast US may be used in patients, in particular those with diaphragm dysfunction. Coupling ultrafast US with CMS opens prospect for a fully non-invasive, non-volitional assessment and follow-up of diaphragm contractility in clinical populations.

Additional information

Data Availability Statement

The data that support the findings of this study are available from the corresponding author upon reasonable request.

Competing interests

JLG is a scientific consultant for Supersonic Imagine, Aix-en-Provence, France. MD received personal fees from Lungpacer.

Fundings

The PhD fellowship of TP is funded by the *Fondation EDF* that is supporting the RespiMyo project, which includes the current study. This study was also supported by the *Association Française Contre Les Myopathies* (AFM).

Author contributions

All authors participated in the conception and design of the study. TP and DB performed experiments. TP, JLG and DB analyzed the data and drafted the original version of the manuscript. All authors critically revised and approved the final version of the manuscript. All persons designated as authors qualify for authorship, and all those who qualify for authorship are listed.

Supporting information

S1. A movie clip, slowed down 40 times, showing pressure signals, M-mode images, and indices derived from ultrafast US is available at the following link: <https://figshare.com/s/fe55c9aa033cb6a42617>.

S2. A movie clip, in real-time, showing B-Mode and M-Mode images during a typical 500-ms ultrafast ultrasound acquisition is available at the following link: <https://figshare.com/s/79fb82dd0361075df33e>

References

- Agostoni E & Rahn H. (1960). Abdominal and thoracic pressures at different lung volumes. *J Appl Physiol* **15**, 1087-1092.
- American Thoracic Society/European Respiratory S. (2002). ATS/ERS Statement on respiratory muscle testing. *Am J Respir Crit Care Med* **166**, 518-624.
- Attali V, Mehiri S, Straus C, Salachas F, Arnulf I, Meininger V, Derenne JP & Similowski T. (1997). Influence of neck muscles on mouth pressure response to cervical magnetic stimulation. *Am J Respir Crit Care Med* **156**, 509-514.
- Bachasson D, Dres M, Nierat M, Doorduyn J, Gennisson J, Hogrel J & Similowski T. (2018). Ultrafast Ultrasound Imaging Grants Alternate Methods for Assessing Diaphragm Function. In *2018 IEEE International Ultrasonics Symposium (IUS)*, pp. 1-4.
- Bachasson D, Dres M, Nierat MC, Gennisson JL, Hogrel JY, Doorduyn J & Similowski T. (2019). Diaphragm shear modulus reflects transdiaphragmatic pressure during isovolumetric inspiratory efforts and ventilation against inspiratory loading. *J Appl Physiol* (1985) **126**, 699-707.
- Bakdash JZ & Marusich LR. (2017). Repeated Measures Correlation. *Front Psychol* **8**, 456.
- Baydur A, Behrakis PK, Zin WA, Jaeger M & Milic-Emili J. (1982). A simple method for assessing the validity of the esophageal balloon technique. *Am Rev Respir Dis* **126**, 788-791.

447

448 Deffieux T, Gennisson JL, Tanter M & Fink M. (2008). Assessment of the mechanical
449 properties of the musculoskeletal system using 2-D and 3-D very high frame rate
450 ultrasound. *IEEE Trans Ultrason Ferroelectr Freq Control* **55**, 2177-2190.

451

452 Dres M & Demoule A. (2020). Monitoring diaphragm function in the ICU. *Curr Opin Crit*
453 *Care* **26**, 18-25.

454

455 Geary CM, Welch JF, McDonald MR, Peters CM, Leahy MG, Reinhard PA & Sheel AW.
456 (2019). Diaphragm fatigue and inspiratory muscle metaboreflex in men and women
457 matched for absolute diaphragmatic work during pressure-threshold loading. *J*
458 *Physiol* **597**, 4797-4808.

459

460 Goligher EC, Laghi F, Detsky ME, Farias P, Murray A, Brace D, Brochard LJ, Bolz SS,
461 Rubenfeld GD, Kavanagh BP & Ferguson ND. (2015). Measuring diaphragm
462 thickness with ultrasound in mechanically ventilated patients: feasibility,
463 reproducibility and validity. *Intensive Care Med* **41**, 642-649.

464

465 Gronlund C, Claesson K & Holtermann A. (2013). Imaging two-dimensional mechanical
466 waves of skeletal muscle contraction. *Ultrasound Med Biol* **39**, 360-369.

467

468 Hamnegaard CH, Wragg S, Kyroussis D, Mills G, Bake B, Green M & Moxham J. (1995).
469 Mouth pressure in response to magnetic stimulation of the phrenic nerves. *Thorax* **50**,
470 620-624.

471

472 Hopkins W. (2002). A new view of statistics: Effect magnitudes. *Retrieved February* **14**,
473 2005.

474

475 Kabitz HJ, Walker D, Walterspacher S & Windisch W. (2007). Controlled twitch mouth
476 pressure reliably predicts twitch esophageal pressure. *Respir Physiol Neurobiol* **156**,
477 276-282.

478

479 Laghi F, Harrison MJ & Tobin MJ. (1996). Comparison of magnetic and electrical phrenic
480 nerve stimulation in assessment of diaphragmatic contractility. *J Appl Physiol* (1985)
481 **80**, 1731-1742.

482

483 Laveneziana P, Albuquerque A, Aliverti A, Babb T, Barreiro E, Dres M, Dubé B-P, Fauroux
484 B, Gea J, Guenette JA, Hudson AL, Kabitz H-J, Laghi F, Langer D, Luo Y-M, Alberto
485 Neder J, O'Donnell D, Polkey MI, Rabinovich RA, Rossi A, Series F, Similowski T,
486 Spengler C, Vogiatzis I & Verges S. (2019). ERS Statement on Respiratory Muscle
487 Testing at Rest and during Exercise. *European Respiratory Journal*, 1801214.

488

489 Loupas T, Powers JT & Gill RW. (1995). An axial velocity estimator for ultrasound blood
490 flow imaging, based on a full evaluation of the Doppler equation by means of a two-
491 dimensional autocorrelation approach. *IEEE Transactions on Ultrasonics*,
492 *Ferroelectrics, and Frequency Control* **42**, 672-688.

493

494 Man WD, Moxham J & Polkey MI. (2004). Magnetic stimulation for the measurement of
495 respiratory and skeletal muscle function. *Eur Respir J* **24**, 846-860.

496

497 Mojoli F, Chiumello D, Pozzi M, Algieri I, Bianzina S, Luoni S, Volta CA, Braschi A &
498 Brochard L. (2015). Esophageal pressure measurements under different conditions of
499 intrathoracic pressure. An in vitro study of second generation balloon catheters.
500 *Minerva Anestesiol* **81**, 855-864.

501

Montaldo G, Tanter M, Bercoff J, Benech N & Fink M. (2009). Coherent plane-wave compounding for very high frame rate ultrasonography and transient elastography. *IEEE Trans Ultrason Ferroelectr Freq Control* **56**, 489-506.

Oppersma E, Hatam N, Doorduyn J, van der Hoeven JG, Marx G, Goetzenich A, Fritsch S, Heunks LMA & Bruells CS. (2017). Functional assessment of the diaphragm by speckle tracking ultrasound during inspiratory loading. *J Appl Physiol (1985)* **123**, 1063-1070.

R Core Team. (2020). R: A Language and Environment for Statistical Computing. R Foundation for Statistical Computing, Vienna, Austria.

Rossi S, Hallett M, Rossini PM & Pascual-Leone A. (2011). Screening questionnaire before TMS: an update. *Clin Neurophysiol* **122**, 1686.

Sandrin L, Catheline S, Tanter M, Hennequin X & Fink M. (1999). Time-resolved pulsed elastography with ultrafast ultrasonic imaging. *Ultrason Imaging* **21**, 259-272.

Shahgholi L, Baria MR, Sorenson EJ, Harper CJ, Watson JC, Strommen JA & Boon AJ. (2014). Diaphragm depth in normal subjects. *Muscle Nerve* **49**, 666-668.

Similowski T, Fleury B, Launois S, Cathala HP, Bouche P & Derenne JP. (1989). Cervical magnetic stimulation: a new painless method for bilateral phrenic nerve stimulation in conscious humans. *J Appl Physiol (1985)* **67**, 1311-1318.

Similowski T, Gauthier AP, Yan S, Macklem PT & Bellemare F. (1993). Assessment of diaphragm function using mouth pressure twitches in chronic obstructive pulmonary disease patients. *Am Rev Respir Dis* **147**, 850-856.

Spiesshoefer J, Henke C, Herkenrath S, Brix T, Randerath W, Young P & Boentert M. (2019). Transdiaphragmatic pressure and contractile properties of the diaphragm following magnetic stimulation. *Respir Physiol Neurobiol* **266**, 47-53.

Teixeira A, Demoule A, Verin E, Morelot-Panzini C, Series F, Straus C & Similowski T. (2007). Superiority of nasal mask pressure over mouth pressure, as a surrogate of diaphragm twitch-related esophageal pressure, in healthy humans. *Respir Physiol Neurobiol* **159**, 236-240.

Tuinman PR, Jonkman AH, Dres M, Shi ZH, Goligher EC, Goffi A, de Korte C, Demoule A & Heunks L. (2020). Respiratory muscle ultrasonography: methodology, basic and advanced principles and clinical applications in ICU and ED patients-a narrative review. *Intensive Care Med* **46**, 594-605.

Ueki J, De Bruin PF & Pride NB. (1995). In vivo assessment of diaphragm contraction by ultrasound in normal subjects. *Thorax* **50**, 1157-1161.

Umbrello M, Formenti P, Longhi D, Galimberti A, Piva I, Pezzi A, Mistraretti G, Marini JJ & Iapichino G. (2015). Diaphragm ultrasound as indicator of respiratory effort in critically ill patients undergoing assisted mechanical ventilation: a pilot clinical study. *Crit Care* **19**, 161.

Vivier E, Mekontso Dessap A, Dimassi S, Vargas F, Lyazidi A, Thille AW & Brochard L. (2012). Diaphragm ultrasonography to estimate the work of breathing during non-invasive ventilation. *Intensive Care Med* **38**, 796-803.

Welch JF, Archiza B, Guenette JA, West CR & Sheel AW. (2018). Sex differences in diaphragmatic fatigue: the cardiovascular response to inspiratory resistance. *J Physiol* **596**, 4017-4032.

Windisch W, Kabitz HJ & Sorichter S. (2005). Influence of different trigger techniques on twitch mouth pressure during bilateral anterior magnetic phrenic nerve stimulation. *Chest* **128**, 190-195.

Wragg S, Aquilina R, Moran J, Ridding M, Hamnegard C, Fearn T, Green M & Moxham J. (1994). Comparison of cervical magnetic stimulation and bilateral percutaneous electrical stimulation of the phrenic nerves in normal subjects. *Eur Respir J* **7**, 1788-1792.

Yan S, Gauthier AP, Similowski T, Macklem PT & Bellemare F. (1992). Evaluation of human diaphragm contractility using mouth pressure twitches. *Am Rev Respir Dis* **145**, 1064-1069.

Tables

Table 1. Within day reliability of twitch transdiaphragmatic pressure ($P_{di_{tw}}$), maximal diaphragm tissue velocity ($V_{di_{max}}$) and diaphragm thickening fraction ($TF_{di_{tw}}$) for all stimulations. SEM, standard error of measurement; ICC, intraclass correlation coefficient; [95% CI], 95% confidence interval.

Variable	Mean (SD)	SEM [95 % CI]	ICC [95 % CI]
$P_{di_{tw}}$ (cmH ₂ O)	11.6 (9.5)	1.55 [1.39 ; 1.75]	0.97 [0.96 ; 0.98]
$V_{di_{max}}$ (mm.s ⁻¹)	5.6 (5.0)	1.89 [1.70 ; 2.13]	0.86 [0.81 ; 0.90]
$TF_{di_{tw}}$ (%)	18.7 (15.6)	10.41 [9.38 ; 11.76]	0.56 [0.43 ; 0.66]

Figures

Figure 1. A. Typical B-Mode image of the diaphragm using conventional ultrasound imaging. Conventional ultrasound uses focused pulses, allowing high image quality but relatively low sampling rate (a few tens per second). The diaphragm can be identified as a three-layers structure superficial to the liver. The echogenic *pleura* and *peritoneum* layers surround the muscular layer of the diaphragm. B. The diaphragm is imaged using the custom ultrafast ultrasound sequence used in this study. Noteworthy, ultrafast ultrasound allows very high frame rate but limited contrast of anatomic structures in comparison to standard US imaging.

Figure 2. Experimental setup and procedure for recording pressure and ultrafast ultrasound images. The participants were asked to bend their neck forward and the central hole of the coil was positioned on the spinous process of the seventh cervical vertebra. Recording of pressure signals was initiated 1000 ms before the onset of ultrasound recording. Cervical magnetic stimulation was applied 100 ms after the onset of a 500-ms ultrafast ultrasound acquisition.

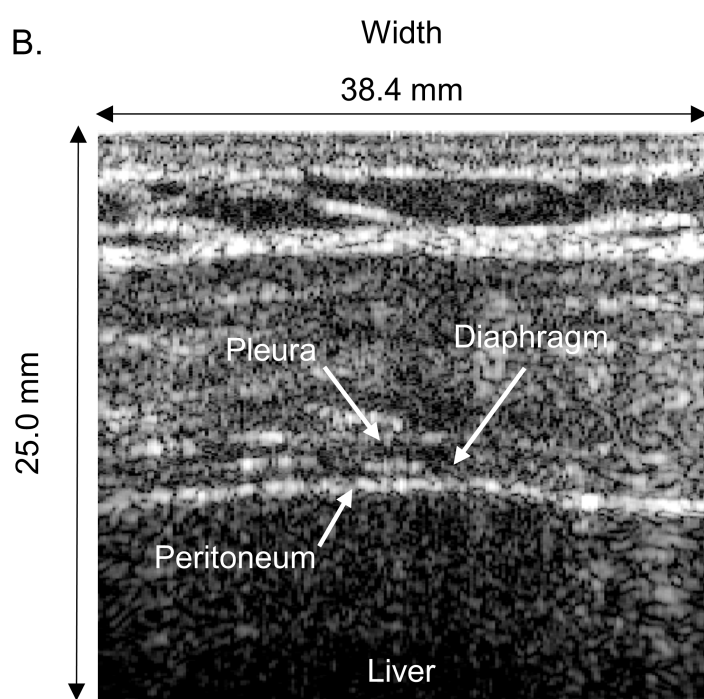
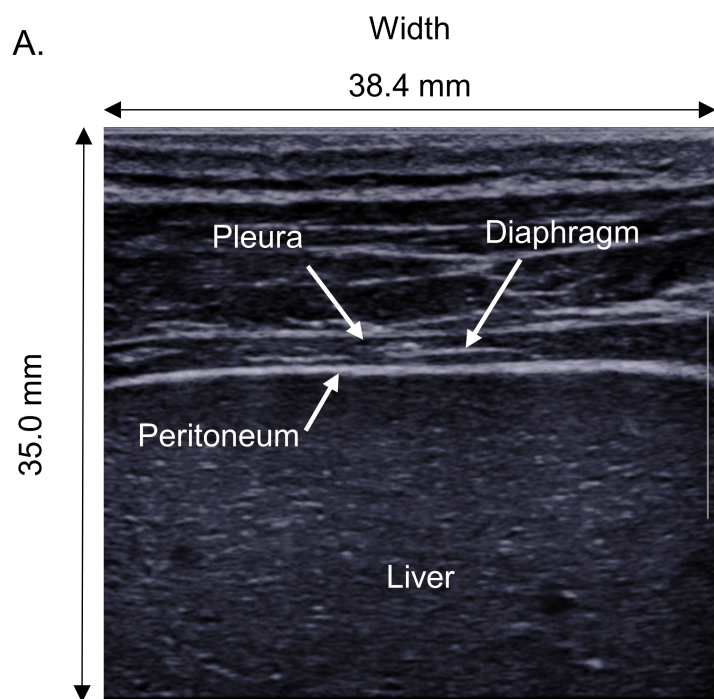
Figure 3. Diaphragm tissue velocity (V_{di}) over time along the longitudinal axis of the ultrasound probe. Cervical magnetic stimulation occurs at 100 ms and is indicated by the grey ribbon.

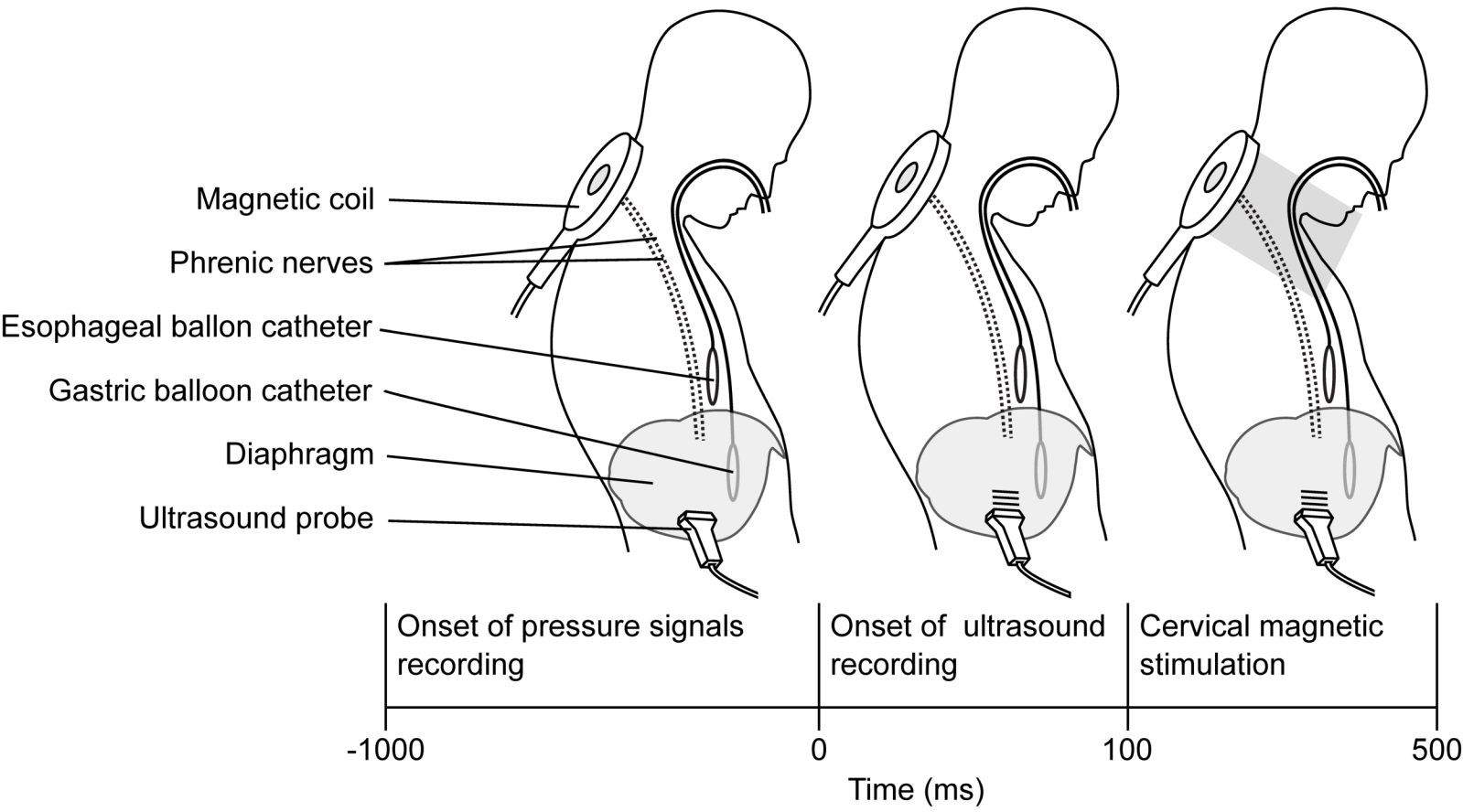
Figure 4. Typical ultrasound and physiological recordings at 40 (left), 70 (center) and 100 % (right) of stimulator intensity. The central pixel of each B-Mode image was used to generate the M-Mode images (upper panel). *Pleura* (dashed) and *peritoneum* (solid) layers displacement are presented in the second panel. Diaphragm tissue velocity (V_{di}) is presented in the third panel. Lastly, the transdiaphragmatic (P_{di}), esophageal (P_{es}) and gastric (P_{ga}) pressures are displayed in the bottom panel. The dotted vertical lines at 100 ms indicate the onset of cervical magnetic stimulation.

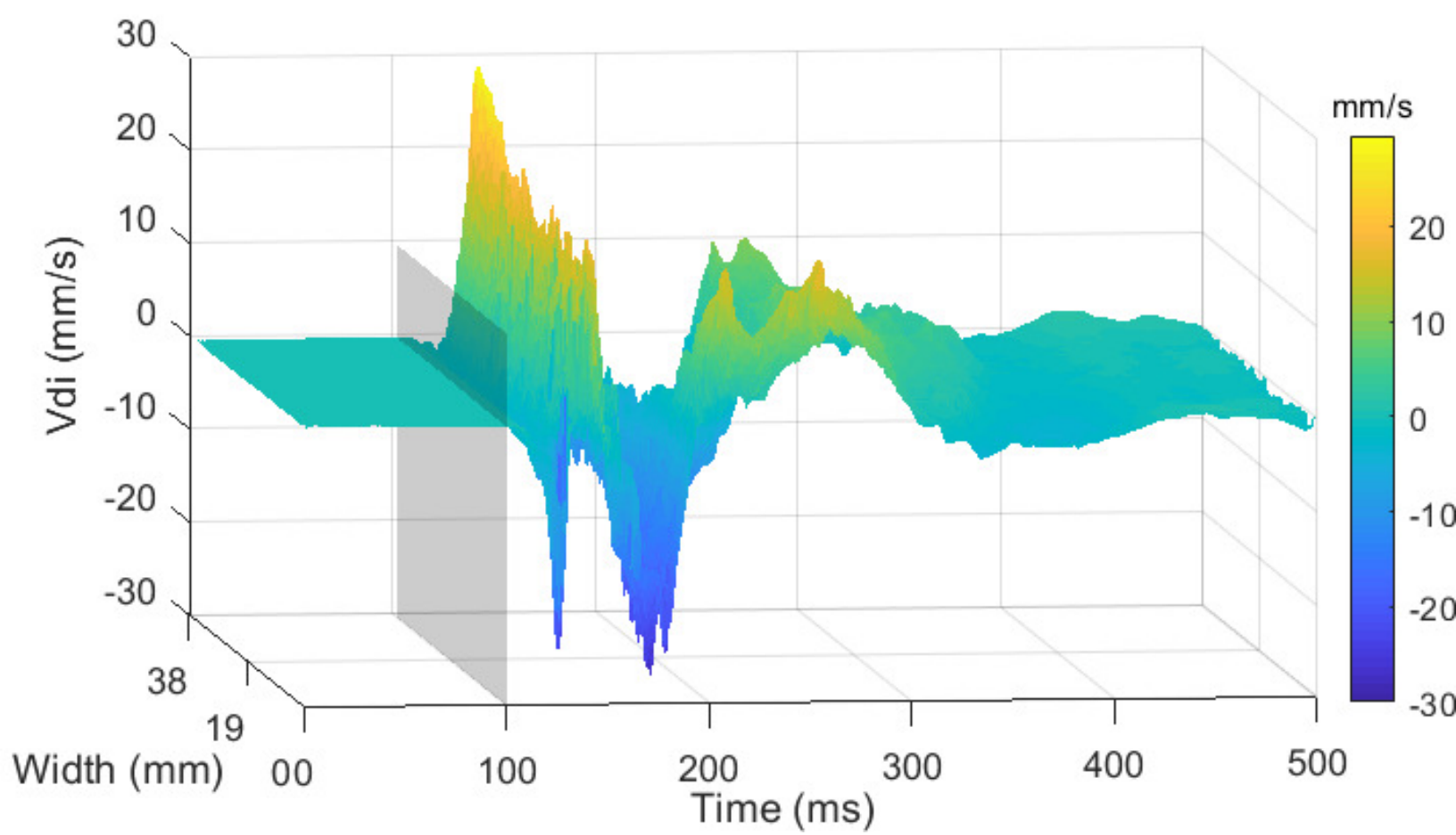
Figure 5. Esophageal (P_{estw} , A.) and gastric (P_{gaw} , B.) twitch pressures at different stimulation intensities. Box plots present first and third quartiles, in addition to the median. The range over which the data spread out is defined by the whiskers.

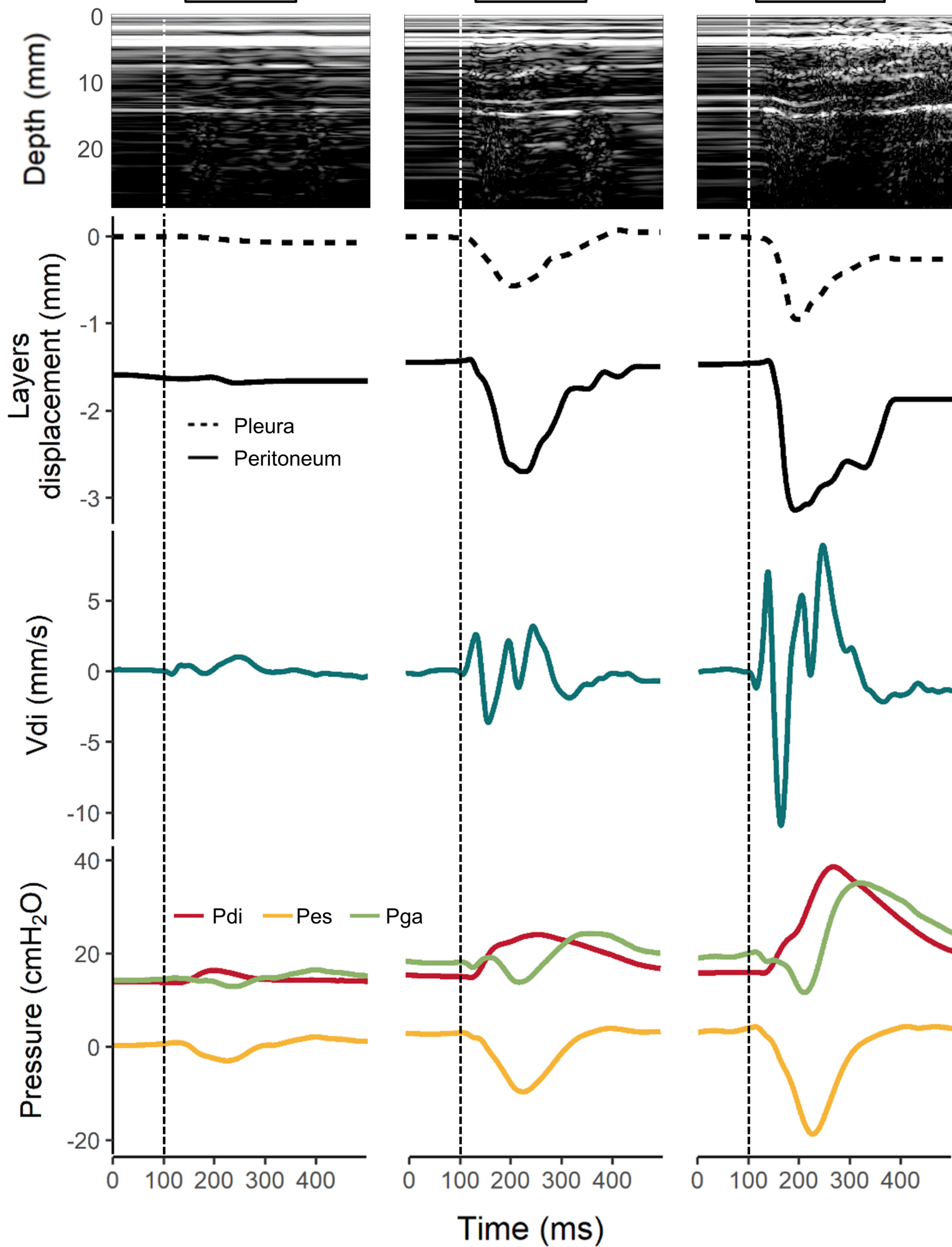
Figure 6. Twitch transdiaphragmatic pressure ($P_{di_{tw}}$, A.), maximal diaphragm tissue velocity ($V_{di_{max}}$, B.), and diaphragm thickening fraction ($TF_{di_{tw}}$, C.) according to stimulation intensities. Box plots present first and third quartiles, in addition to the median. The range over which the data spread out is defined by the whiskers. Repeated measure ANOVAs were used to assess the effect of stimulation intensity on $P_{di_{tw}}$, $V_{di_{max}}$, and $TF_{di_{tw}}$. Tukey's *post-hoc* tests were conducted if a significant main effect of intensity was found. *, significant difference with the preceding stimulation intensity (i.e. -10 %); #, significant difference with the second preceding stimulation intensity (i.e. -20 %). Averaged data points for each participant are displayed for $P_{di_{tw}}$ (D.), $V_{di_{max}}$ (E.), and $TF_{di_{tw}}$ (F.). Red points on panels D, E, and F indicate supramaximality for the given parameter.

Figure 7. Averaged data points for each participant regarding the relationships between twitch transdiaphragmatic pressure ($P_{di_{tw}}$) and maximal diaphragm tissue velocity ($V_{di_{max}}$, A.) and between $P_{di_{tw}}$ and diaphragm thickening fraction ($TF_{di_{tw}}$, B.).

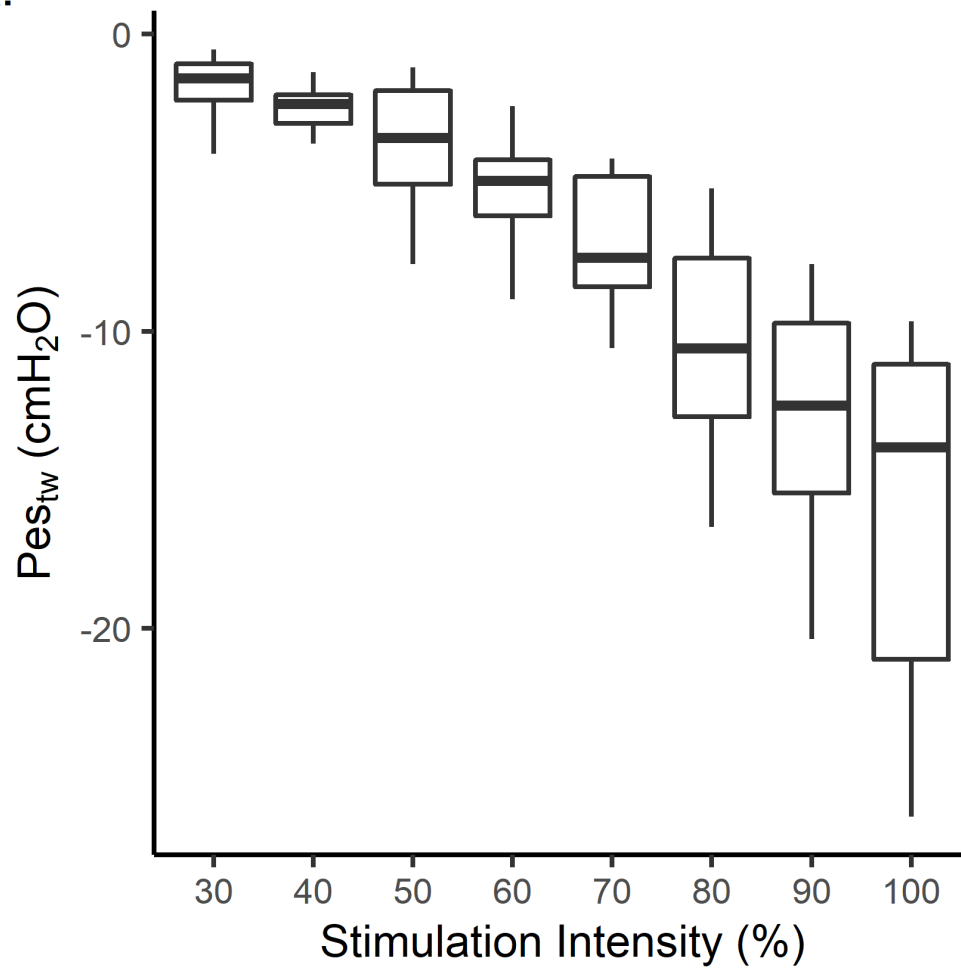




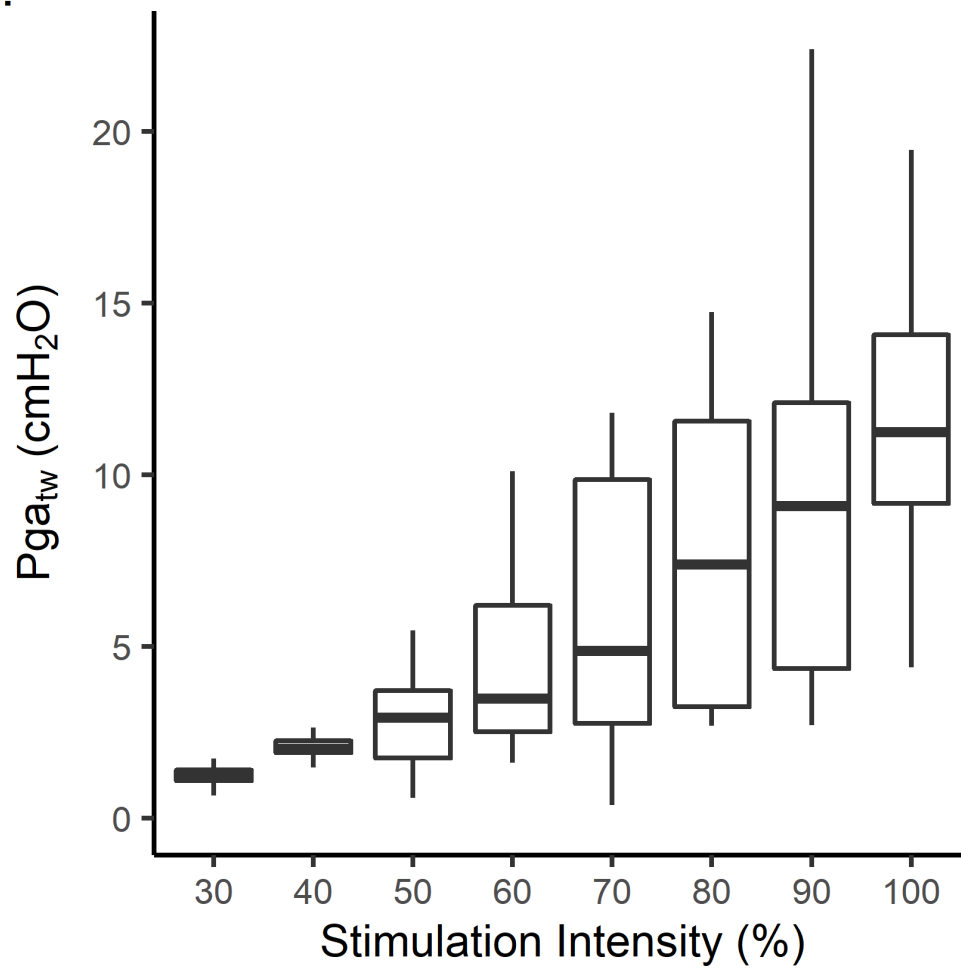


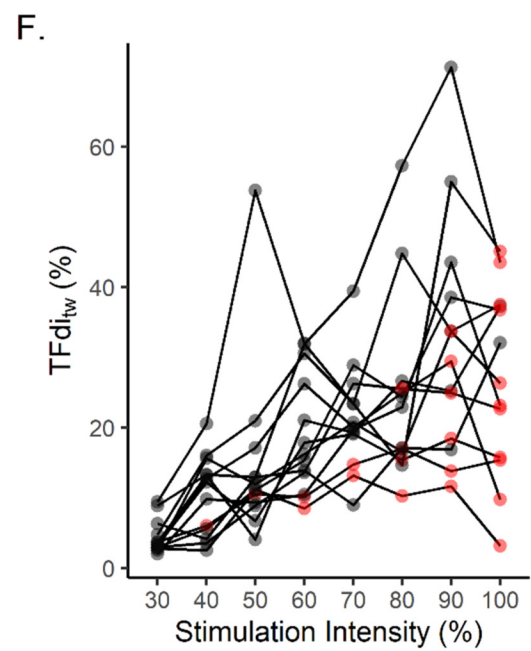
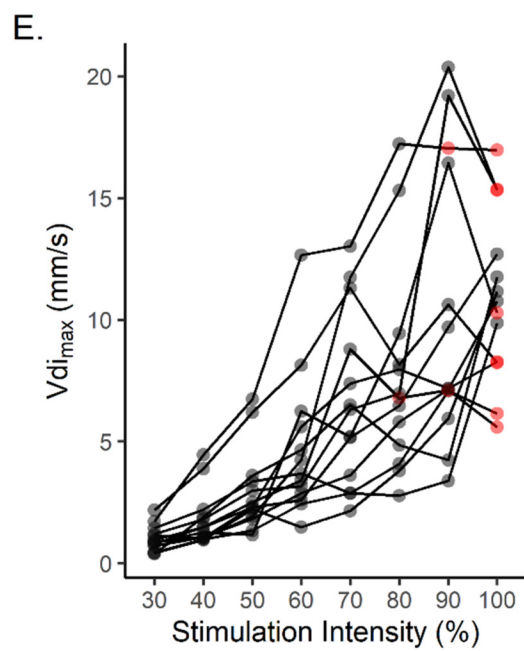
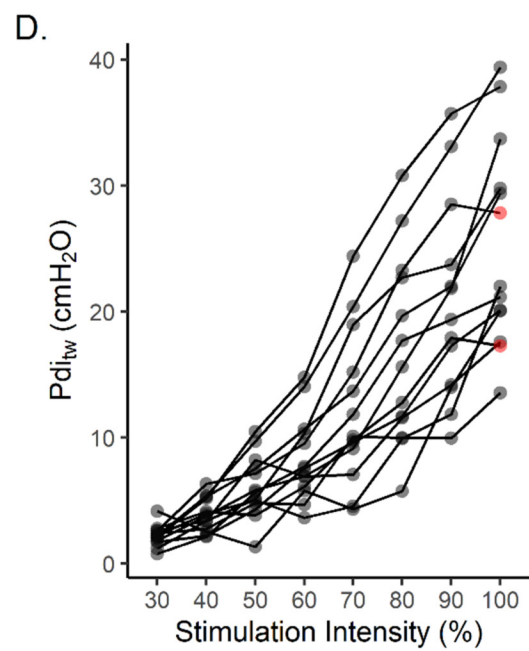
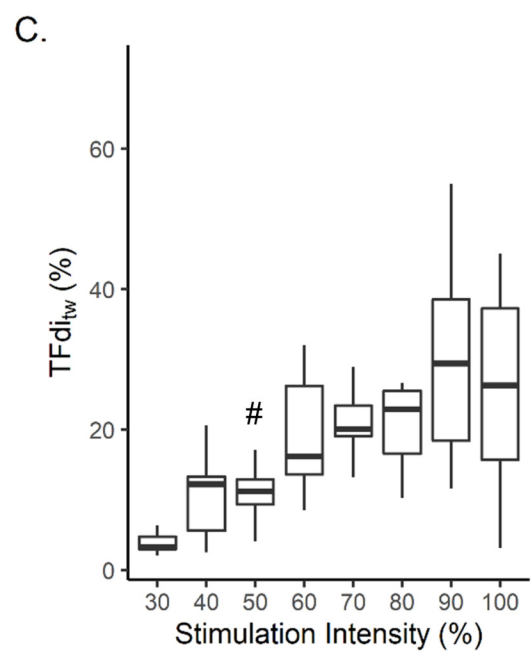
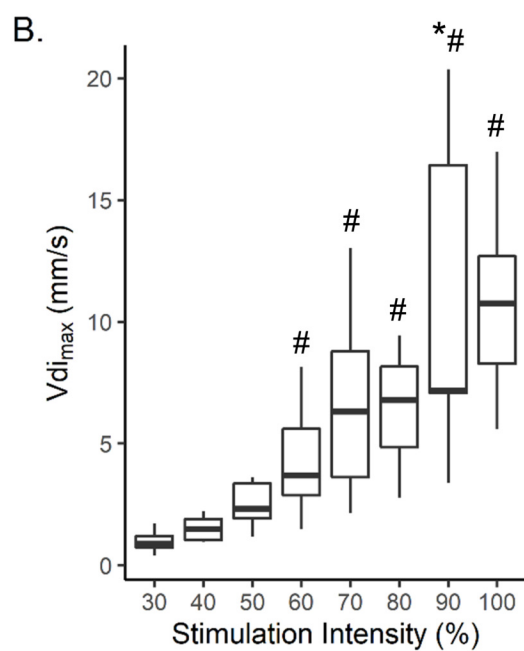
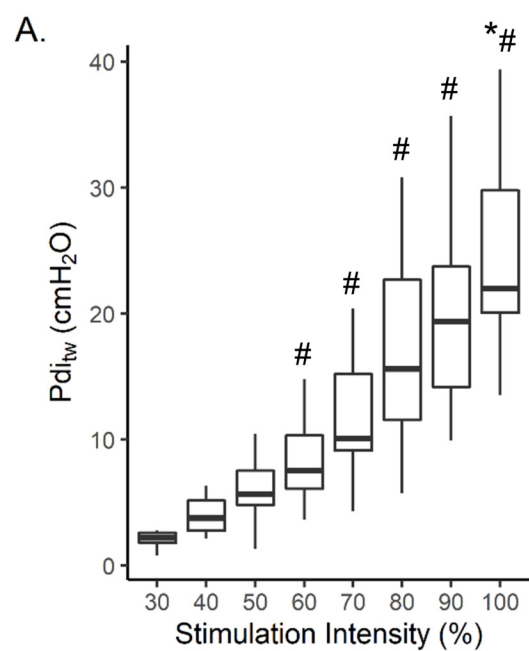
40 %**70 %****100 %**

A.

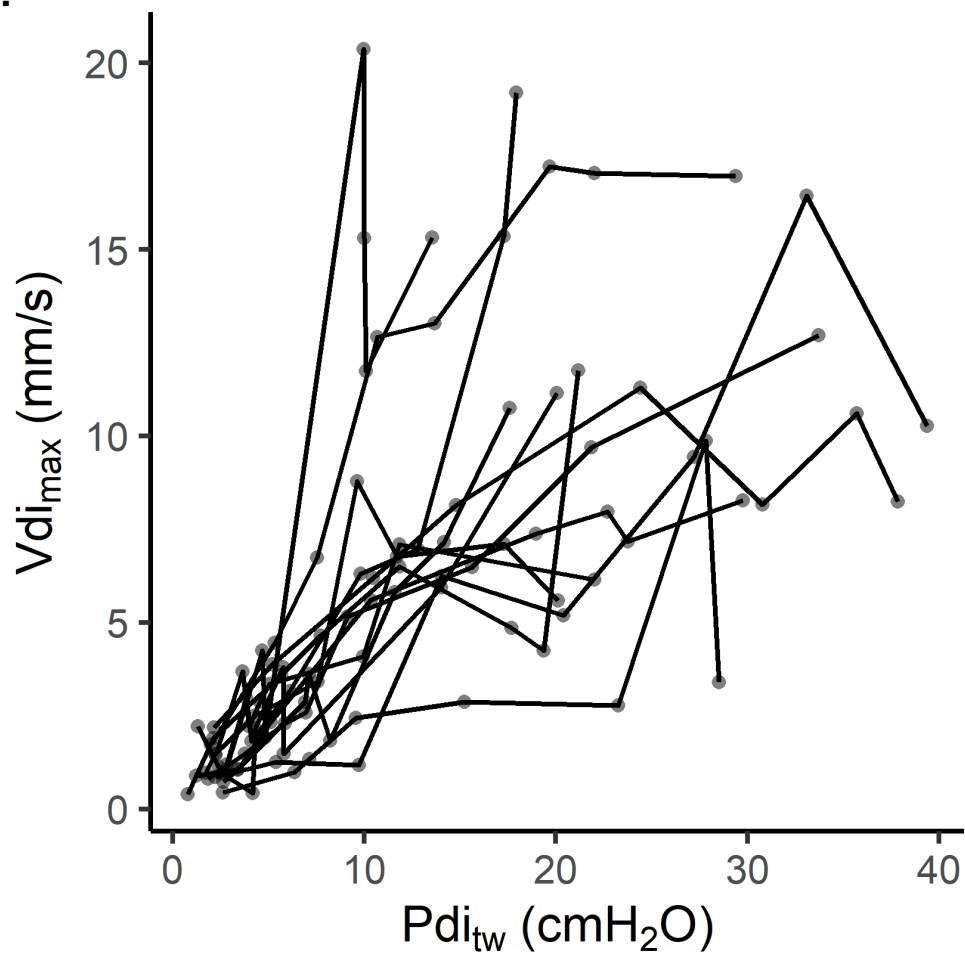


B.





A.



B.

